Journal of Chromatography B, 878 (2010) 2719–2725

Contents lists available at ScienceDirect

Journal of Chromatography B

journal homepage: www.elsevier.com/locate/chromb

Process optimisation for anion exchange monolithic chromatography of 4.2 kbp plasmid vaccine (pcDNA3F)

Clarence M. Ongkudon*, Michael K. Danquah

Bio Engineering Laboratory, Department of Chemical Engineering, Faculty of Engineering, Monash University, Clayton Campus, Wellington Road, Clayton, Victoria 3800, Australia

ARTICLE INFO

Article history:
Received 1 July 2010
Accepted 12 August 2010
Available online 19 August 2010

Keywords:
Process optimisation
Anion exchange
Monolithic chromatography
Plasmid DNA
pcDNA3F

ABSTRACT

Anion exchange monolithic chromatography is increasingly becoming a prominent tool for plasmid DNA purification but no generic protocol is available to purify all types of plasmid DNA. In this work, we established a simple framework and used it to specifically purify a plasmid DNA model from a clarified alkaline-lysed plasmid-containing cell lysate. The framework involved optimising ligand functionalisation temperature (30–80 °C), mobile phase flow rate (0.1–1.8 mL/min), monolith pore size (done by changing the porogen content in the polymerisation reaction by 50–80%), buffer pH (6–10), ionic strength of binding buffer (0.3–0.7 M) and buffer gradient elution slope (1–10% buffer B/min). We concluded that preferential pcDNA3F adsorption and optimum resolution could be achieved within the tested conditions by loading the clarified cell lysate into 400 nm pore size of monolith in 0.7 M NaCl (pH 6) of binding buffer followed by increasing the NaCl concentration to 1.0 M at 3%B/min.

1. Introduction

Anion-exchange chromatography (AEC) remains one of the most prominent methods in plasmid DNA (pDNA) purification due to its rapid separation, easy sanitisation, no organic solvent requirements and wide selection of available stationary phases [1]. In terms of quality and recovery, consistent results have been achieved at different scales [2]. AEC is based on the interaction between negatively charged phosphate groups of plasmid and positively charged stationary matrix [3]. A buffer containing sodium chloride salt can be used as the eluting buffer and a gradient elution can be performed at a specific slope (% eluting buffer/min) for optimum resolution [4]. Molecules with lower charge densities should elute first followed by high negatively charged molecules, a trend, which is attributed to plasmid chain length and conformation [5].

The purification of large biomolecules, such as plasmids is obstructed by the performance of conventional chromatographic supports with a small particle pore diameter. Most of these chromatographic supports are geared towards high adsorption capacities of small molecules such as proteins and peptides. In columns packed with such particles, plasmids greater than 100 nm adsorb predominantly on the outer surface of the particles and this leads to low binding capacities [6]. A monolith is a continuous phase consisting of a piece of highly porous organic or inorganic solid material. The most essential feature of this support is that all the mobile phase is forced to flowthrough its large pores. As a consequence, mass transport is steered by convection; reducing the long diffusion time required by particle-based supports [7]. The pore size of the monolith plays an important role in providing spaces for both ligand attachment and plasmid mobility. Based on a previous study, it is speculated that bimodal pore sizes of 0.008 and 0.5 μm can provide the optimum condition for ligand coupling, plasmid binding and plasmid retention [8]. The pore size of the monolith can be altered by varying the composition of the reactants and porogens. One of the most studied monolithic materials is silica based monolith which has been reported in [9–11]. Silica based monolith has been used in analytical chromatography and resulted in a significantly short processing time compared to conventional packed bed column [12]. Another type of monolithic material is polymethacrylate based monolith which is the type of chromatographic column used in this work. Polymethacrylate monoliths are especially useful for large-scale purification of large biomolecules owing to its enhanced mass transfer properties, pressure and flow, specific permeability, morphological and structural stability [13].

To optimise the ligand coupling on polymethacrylate, crucial parameters such as temperature, reaction time and pH can be optimised. Generally, the ligand coupling rate increases with temperature according to the Arrhenius equation [14]. At high pH values, the epoxy group of polymethacrylate is more reactive than

* Corresponding author. Tel.: +61 401338799; fax: +61 399055686.
E-mail addresses: clarence.ongkudon@monash.edu, clarence.ongkudon@eng.monash.edu.au (C.M. Ongkudon).

1570-0232/$ – see front matter © 2010 Elsevier B.V. All rights reserved.
doi:10.1016/j.jchromb.2010.08.011

that at low pH values. However, the maximum pH value is limited by the ligand stability which in most cases affected by deactivation, leaching and aggregation. Using high ionic strength binding buffers can also improve the ligand coupling on polymethacrylate but extra care has to be taken when using highly ionic binding buffers since they may lead into disruption of the covalent linkage of the polymethacrylate or monolith shrinkage.

pH can greatly alter the monolith charge density and thereby affect the success of the plasmid purification [8]. In this work, different pH values were tested for optimal plasmid purification. Effect of pH on the overall plasmid charge and ligand charge densities was analysed by Zeta potential analyser. Plasmid purity, recovery and peak resolution are coherently influenced by chromatographic residence time [8]. Residence time can be altered by manipulating buffer flow rate and column length. Generally at low flow rates and high column lengths, separation will be more efficient due to an increase in retention time of the solute of interest. At low flow rates however, the peak width may be broadened resulting in low plasmid recovery and low resolution. Therefore, an optimisation of buffer flow rate is necessary and a mathematical study can be carried out to assess the trade-off between plasmid purity and recovery [15].

2. Materials and methods

Ethylene glycol dimethacryalte (EDMA) (*M*w 198.22, 98%), glycidyl methacrylate (GMA) (*M*w 142.15, 97%), cyclohexanol (*M*w 100.16, 99%), 1-dodecanol (*M*w 186.33, 98%), AIBN (*M*w 164.21, 98%), MeOH (HPLC grade, *M*w 32.04, 99.93%), DEA (*M*w 73.14, 99%) were purchased from Sigma–Aldrich. NaCl (Amresco, *M*w 58.44, 99.5%), agarose (Promega), SDS (Amresco, *M*w 288.38, 99.0%), Na_2CO_3 (SPECTRUM, *M*w 105.99, 99.5%), Tris (Amresco, Mw 121.14, 99.8%), EDTA (SERVA, *M*w 292.3, AG), EtBr (Sigma, *M*w 394.31, 10 mg/mL), 1 kbp DNA marker (BioLabs, New England), Wizard plus SV Maxipreps (Promega).

2.1. Model plasmid vaccine

E coli DH5α carrying plasmid measles vaccine (pcDNA3F) was provided by Dr. Diane Webster of School of Biological Sciences, Monash University, Australia.

2.2. Cell line propagation

10 μL of transformed cells (*E. coli* DH5α-pcDNA3F) was cultured in LB–agar–ampicillin plate at 37 °C overnight. A single *E. coli* DH5α-pcDNA3F colony was picked from the LB–agar–ampicillin plate and subcultured with 250 mL of LB media containing 100 μg/mL ampicillin and 0.5% (v/v) glycerol at 37 °C overnight under 200 rpm shaking. Subsequently, 2 mL of the culture was inoculated into 1000 mL medium containing 100 μg/mL ampicillin and 0.5% (v/v) glycerol. The fermentation was run at 37 °C under 200 rpm shaking and was harvested at 15 h post inoculation.

2.3. Preparation of E. coli DH5α-pcDNA3F cleared lysate

5 g of frozen *E. coli* DH5α-pcDNA3F bacterial cell paste were thawed at 37 °C and resuspended in 50 mL of 0.05 M Tris–HCl, 0.01 M EDTA, pH 8 buffer. The resuspended cells were homogenously mixed with 50 mL of lysis solution (0.2 M NaOH, 1% SDS) for 5 min by gently swirling the mixture. Neutralisation was performed by the addition of 75 mL 3 M CH_3COOK at pH 5.5 to the lysed cell suspension for 5 min. The mixture of pDNA-containing cleared lysate and the precipitated impurities, mainly gDNA were separated by centrifugation at 4600 rpm for 30 min.

2.4. Synthesis and amino functionalisation of poly(GMA–EDMA) monolithic column

The monolith was prepared via free radical co-polymerisation of EDMA and GMA monomers. EDMA/GMA mixture was combined with alcohol-based bi-porogen solvents in the proportion 20/10/60/10 (GMA/EDMA/cyclohexanol/1-dodecanol) making a solution with a total volume of 2 mL. AIBN (1% weight with respect to monomer) was added to initiate the polymerisation reaction. The polymer mixture was sonicated for 15 min and sparged with N_2 gas for 15 min to expel dissolved O_2. The mixture was gently transferred into a conical 0.8 cm × 4 cm polypropylene column (BIORAD) sealed at the bottom end. The top end was sealed with a parafilm sheet and placed in a water bath for 18 h at 60 °C. The polymer resin was washed to remove all porogens and other soluble matters by flowing through the column with methanol for 20 h at room temperature. The polymer was washed with deionised water at 0.3 mL/min for 60 min followed by a solution containing 17 mM DEA, 20 mM Na_2CO_3 and 3 mM NaCl at 0.1 mL/min for 20 h in a 60 °C waterbath. The resulting functionalised polymer was washed with deionised water.

2.5. Preparation of suspended poly(GMA–EDMA) particles for Zeta potential analysis

Suspended poly(GMA–EDMA) particles for Zeta potential analysis was prepared by dispersion polymerisation. A 50 mL mixture of GMA, EDMA, cyclohexanol, 1-dodecanol (20:10:60:10 v/v respectively) and 0.15 g AIBN was prepared at room temperature in a shake flask. The polymer mixture was sonicated for 15 min and sparged with N_2 gas for 15 min. The top end was sealed with a parafilm sheet and placed in an incubater for 24 h at 60 °C under 300 RPM shaking. The polymerised poly(GMA–EDMA) was transferred into a shake flask containing 200 mL methanol for 15 h at 200 rpm. At this stage, most of the polymer existed as finely suspended particles (<1 μm). The suspended polymer was centrifuged and resuspended in a 50 mL solution containing 25 mM Tris–HCl, 2 mM EDTA and 0.005 M NaCl at pH 8.

2.6. Chromatographic purification of pcDNA3F

The conical column containing 2 mL of functionalised monolithic resin was connected and configured to BIORAD HPLC system. Before the chromatography was performed, column equilibration was done with buffer A (25 mM Tris–HCl, 2 mM EDTA, 0.2 M NaCl, pH 7) at 0.6 mL/min until a constant UV baseline was achieved. 1 mL of clarified cell lysate was diluted (0.5×) with buffer A and applied at 0.6 mL/min. A washing step was done with 15 column volumes (CVs) buffer A at 0.6 mL/min to completely remove the unbound and weakly retained molecules especially proteins. The elution of pcDNA3F was done by mixing buffer A with buffer B (25 mM Tris–HCl, 2 mM EDTA, 1.0 M NaCl, pH 7) at 4% B/min. Column cleaning was performed by washing the column with 50 CVs of a solution containing 0.5 M NaOH and 2 M NaCl followed by 50 CVs of 70% EtOH solution. The column was then regenerated with 10 CVs of buffer B.

2.7. Plasmid DNA qualitative and quantitative analyses

Standard pcDNA3F was prepared using Wizard plus SV Maxipreps according to the manufacturer's instructions (Promega). The concentration of the plasmid was determined via UV absorbance at 260 nm. An absorbance value of 1.0 unit measured at 260 nm represents 50 mg/L double stranded DNA. Nature and size of the plasmid were determined by ethidium bromide agarose gel electrophoresis using 1 kbp DNA ladder. The gel was made up of 50× diluted TAE

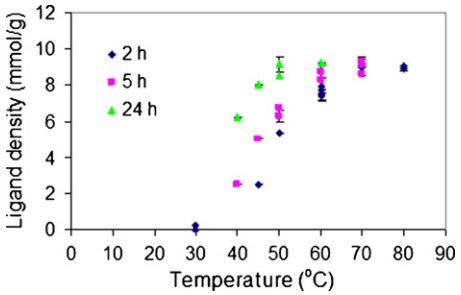

Fig. 1. Diethylamine densities measured at different functionalisation temperatures and incubation periods. Ligand densities were calculated based on the difference in dry weights of the polymer before and after functionalisation was performed. Functionalisation was done at 2 h (rhombus), 5 h (square) and 24 h (triangle) of incubation periods between 30 and 80 °C.

buffer (242 g Tris base, 57.1 mL acetic acid, 9.305 g EDTA), stained with 3 μg/mL ethidium bromide and run for 2 h at 66 V. The gel was photographed with a gel analyser (BIORAD, Universal Hood II, Italy). The hydrodynamic size distribution and electrokinetics behaviour of plasmid and functionalised poly(GMA–EDMA) as well as their interactions at different conditions were assessed using Zetasizer and Zeta potential analyser according to the manufacturer's instructions (Malvern Instruments).

3. Results and discussion

3.1. Effect of temperature on rate of ligand functionalisation

The dependency of DEA and poly(GMA–EDMA) coupling on reaction temperature can be checked using Arrhenius equation.

$$k = Ae^{-E_a/RT} \quad (1)$$

where k is the effective ligand coupling rate (mol/s) obtained by measuring ligand densities every minute for 1 h, A is total number of DEA and poly(GMA–EDMA) collisions (mol/s), E_a is activation energy of poly(GMA–EDMA)–DEA (J/mol), R is gas constant (8.314 J/mol K), and T is temperature (K). Taking ln of Eq. (1) yields the following equation:

$$\ln k = \left(\frac{-E_a}{R}\right)\frac{1}{T} + \ln A \quad (2)$$

By fitting Eq. (2) into experimental data, the correlation factor (R^2) was calculated as 0.99, A value was 8.235×10^{13} mol/s and activation energy for ligand coupling was 1.24×10^5 J/mol.

At high temperatures, the ligand functionalisation rate was high leading to a shorter reaction time and *vice versa* (as seen in Fig. 1). At very high temperatures however, the monolith pore structures became uneven leading to reduced binding capacities and resolution. In this study we found that the optimum temperature for ligand functionalisation was at 60 °C.

3.2. Optimisation of mobile phase flow rate

During chromatography, the movement of plasmids through monolith is influenced by diffusion, adsorption and convection of plasmids inside the monoliths. These factors are related to linear velocity of mobile phase as suggested by the Van Deemter equation. By running plasmid samples at different flow rates, the height equivalent to theoretical plate (HETP) can be calculated and used to determine the optimum flow rate. As depicted in Fig. 2, the optimum linear velocity is at 0.6 m/min which is equivalent to a volumetric flow rate of 0.6 mL/min. Under this condition, the resulting chromatographic peaks are sharp, symmetrical and band broadening is minimised. At flow rate <0.6 mL/min, plasmids spend more time in the monolith and start to diffuse out from the centre to the edges thus leading to band broadening and reduced chromatographic efficiency. At flow rate >0.6 mL/min, band broadening are more complicated. Besides the differences in residence time between plasmids in mobile phase and plasmids in stationary phase, Zochling et al. [16] suggested that band broadening occurring at high flow rates is also attributed to the stretching of the plasmid DNA caused by flow-induced shear stress [17]. Further to the flow-induced elongational stress, fewer amounts of plasmids are bound per unit area of the anion exchange surface thus resulting in lower plasmid yields.

We also propose herein that, as a result of a very high flow rate-induced shear stress, plasmids may become nicked thus leading to lower supercoiled plasmid DNA yields [17,18]. Shear-induced plasmid elongational and degradation are complex events and current understanding of the effects of shear rate on plasmid shapes does not provide a final answer to these proposed phenomena. In view of this, it is prudent to investigate the molecular mechanism of effect of shear stress on plasmid shape and stability to better control the monolithic chromatography of plasmids and comply with regulatory standards.

3.3. Optimisation of pore size

The chromatographic resolution of plasmid DNA significantly depends on the active surface accessibility. In this case the active surface is actually the monolith pore surfaces. The channels should be large enough to allow penetration of large plasmid DNAs (>100 nm) and at the same time to separate other impurities of smaller sizes (<100 nm). If the pore size is too small, not only the resolution is poor but also the back pressure is high too. The first step to determine the optimum pore size of the monolith for plasmid purification is to measure the hydrodynamic size of double stranded supercoiled plasmid DNA by dynamic light scattering method. Based on the size of the plasmid, the monolith pore size can then be formed according to methods described by Danquah and Forde [19]. Further optimisation of pore size can be done for a greater plasmid resolution by fine tuning the amount of porogen in the monolith preparation.

Based on Fig. 3, the mean hydrodynamic diameter of the model plasmid pcDNA3F as measured by the Zetasize analyser (Malvern Instruments) is 137 nm. Therefore, the monolith pore size should at least be 137 nm. In a real application, the monolith pore size is much larger than the plasmid. This is to compensate with the high mobile phase flow rate and different molecules that exist in the clarified plasmid-containing cell lysate. To optimise the mono-

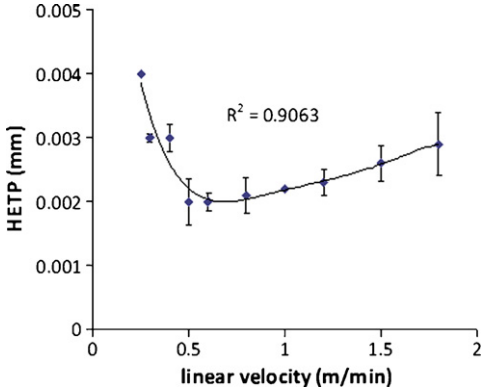

Fig. 2. Effect of flow rate on column efficiency. Buffer A (25 mM Tris–HCl, 2 mM EDTA, 0.2 M NaCl, pH 7). Buffer B (25 mM Tris–HCl, 2 mM EDTA, 1.0 M NaCl, pH 7). Sample: 0.5 mL of clarified alkaline-lysed cell lysate. Washing, 30 CVs of buffer A; gradient elution, 4% B/min.

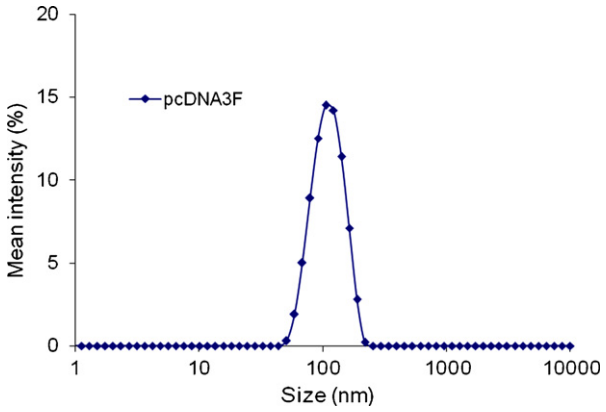

Fig. 3. Hydrodynamic size distribution of plasmid pcDNA3F. Mean size is ~137 nm in 25 mM Tris–HCl, 2 mM EDTA and 0.005 M NaCl at pH 8.

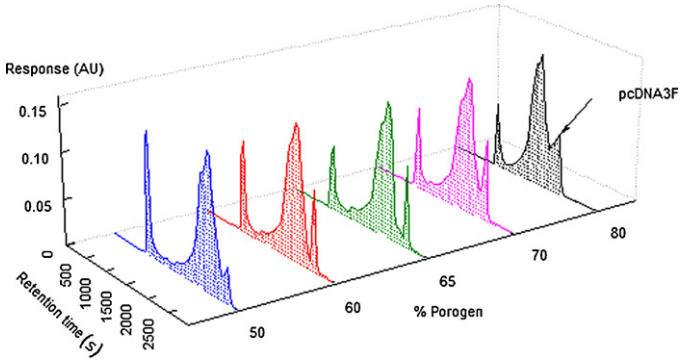

Fig. 4. Effect of porogen:monomer ratio on plasmid resolution. Flow rate 0.6 mL/min. Buffer A (25 mM Tris–HCl, 2 mM EDTA, 0.2 M NaCl, pH 7). Buffer B (25 mM Tris–HCl, 2 mM EDTA, 1.0 M NaCl, pH 7). Sample: 0.5 mL of clarified alkaline-lysed cell lysate. Washing, 30 CVs of buffer A; gradient elution, 4% B/min [19].

lith pore size for plasmid pcDNA3F purification, different porogen contents in monolith preparation were tested. The effects of porogen on plasmid resolution and monolith pore size are shown in Figs. 4 and 5.

In general, smaller pore size results in the solute not entering the pores thus larger pore size is needed to cater for both ligand attachment and plasmid mobility. A decreasing trend of plasmid retention with increasing porogen content is observed in Fig. 4. This can be explained by analysing the internal structures of the monolith in Fig. 5. At 40% porogen, the modal pore diameter is 115.7 nm which is vaguely smaller than pcDNA3F. As a result of this internal resistance, the plasmids may take longer time to pass through the pores by flow-induced elongational stress and may co-elute with other molecules of smaller size. Fractions of the plasmids may remain within the pores or elute at a later time thus resulting in lower plasmid yield and band broadening as depicted in Fig. 4. At 80% porogen, the modal pore size is 875.6 nm which is 8 times larger than the size of pcDNA3F. At this point, plasmid resolution may become less dependent on monolith pore size and therefore depends solely on buffer gradient elution for separation. It is also important to note that at a substantially large pore size, the surface area is greatly reduced thus resulting in a lower binding capacity. This affects the overall positive charge density of the matrix which in turn affects the electrostatic interaction and plasmid separation. In this study, the optimum monolith pore size for pcDNA3F resolution occurs at 65% porogen. This value corresponds to a pore size of approximately 400 nm according to Danquah and Forde [19].

3.4. Effect of NaCl in binding buffer on plasmid retention and binding capacity

When a clarified plasmid-containing bacterial lysate is loaded into an anion exchange monolithic column, a strong competition occurs between plasmids and negatively charged impurities for the anion exchange matrix. This leads to reduced plasmid binding capacity and low plasmid recovery during elution. One way of minimising the adsorption of lower charged impurities onto the matrix is by increasing the ionic strength of binding buffer by means of increasing NaCl concentration. Theoretically, the optimum NaCl concentration of binding buffer can be defined as the point where all impurities carry zero net surface charge leaving only plasmids with net negatively charged surface. Under this circumstance, the monolith internal surface area can be fully utilised for plasmid adsorption.

To obtain the relative surface charge of a particle, we measured the Zeta potential of the particles which is defined as the electric potential at a particular distance off the particle surface called the hydrodynamic slip plane [20]. According to Fig. 6, plasmid pcDNA3F remains negatively charged at 2 M NaCl whilst proteins and RNAs are neutralised at 0.25 and 1.0 M NaCl respectively. We predicted that at a NaCl concentration of ~1.0 M in loading buffer, majority of the plasmids would stay within the monolith matrix leaving all impurities especially proteins and RNA in the flowthrough. We also hypothesised that plasmid yield would not be affected considering the same amount of sample loaded into the monolith. To verify these hypotheses, four chromatographic runs were performed at 0.3, 0.4, 0.5 and 0.7 M NaCl in loading/binding buffer. The elution step was initiated at 5 min post loading by gradient elution up to 1.0 M NaCl at 4% B/min. The chromatograms of the analyses are shown in Fig. 7. Generally the retention time was high at low ionic strength of binding buffer and *vice versa*. A decreasing trend of RNA yield with increasing ionic strength of binding buffer was observed between 0.3 and 0.7 M NaCl. RNA adsorption was virtually eliminated at 0.7 M which was slightly lower than the predicted value of 1.0 M.

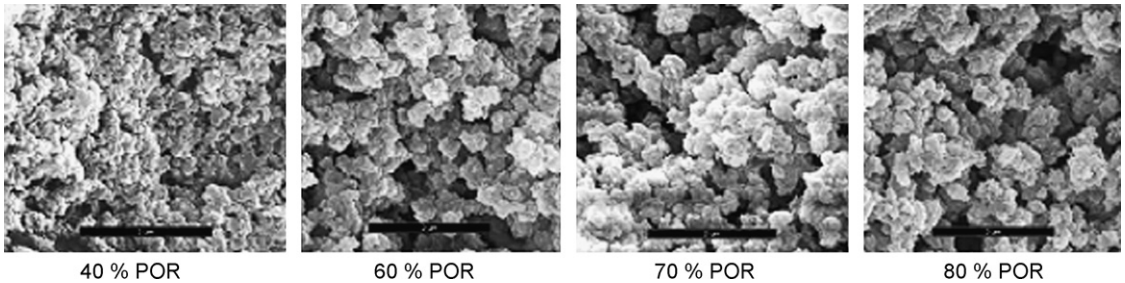

Fig. 5. SEM photographs of poly(GMA–EDMA) polymerised at different porogen:monomer ratios. Polymerisations were carried out with a constant monomer ratio (EDMA/GMA) of 40/60; porogen concentrations of 40%, 60%, 70% and 80%; polymerisation temperature of 60 °C; AIBN concentration of 1% (w/w) with respect to monomers. Microscopic analysis was performed at 15 kV. POR:porogen.

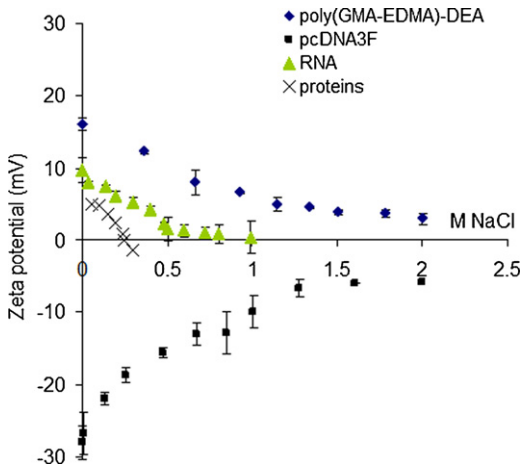

Fig. 6. Effect of buffer's ionic strength on the Zeta potential of pcDNA3F and poly(GMA–EDMA)–DEA. Base buffer (25 mM Tris–HCl, 2 mM EDTA, 0 M NaCl, pH 7). Each data point represents the average of three replicates.

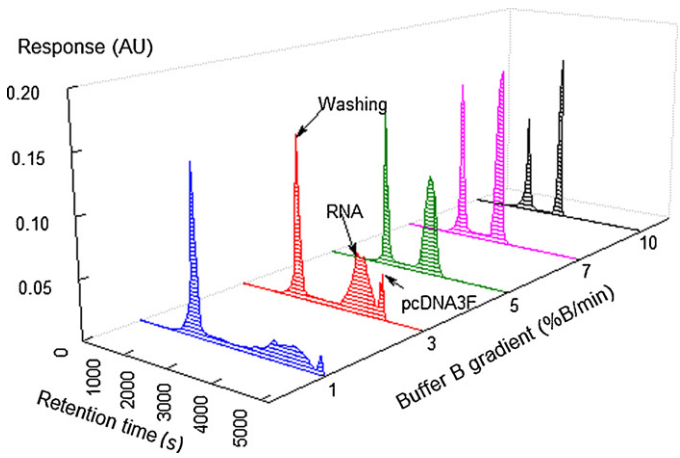

Fig. 8. Effect of buffer B gradient on plasmid resolution. Flow rate 0.6 mL/min. Buffer A (25 mM Tris–HCl, 2 mM EDTA, 0.2 M NaCl, pH 7). Buffer B (25 mM Tris–HCl, 2 mM EDTA, 1.0 M NaCl, pH 7). Sample: 0.5 mL of clarified alkaline-lysed cell lysate. Washing, 30 CVs of buffer A.

The trend of plasmid yield however, did not quite agree with the hypothesis since plasmid yield seemed to decrease slightly with increasing NaCl concentration in binding buffer. This trend can be explained from the condensation theory which postulates that upon neutralisation of negatively charged phosphate groups in the DNA backbone, the repulsive forces are weakened thus allowing the DNA to collapse into compact forms [17,21]. We also propose that at a high ionic strength of binding buffer, the amount of plasmid DNA bound per unit area of the anion exchange surface is reduced due to decreased electrostatic attraction exerted by the matrix surface. As a result of this compaction, the effective hydrodynamic diameter of the DNA is decreased and the loosely retained molecules can easily flowthrough the monolith pores.

3.5. Optimisation of gradient elution

In ion exchange monolithic chromatography, the major mechanism that contributes to plasmid separation is attributed to size exclusion and close vicinity electrostatic interaction between the plasmid and ligand. Plasmid elution is done by increasing the ionic strength (e.g. NaCl concentration) of the mobile phase. As discussed previously, the presence of NaCl in a mobile phase reduces the effective net charge of both plasmid and ligand. NaCl also affects the hydrodynamic size of plasmid and other impurities such as RNAs and proteins. To effectively separate plasmid DNA from contaminating species, NaCl concentration was increased gradually and each species was eluted from the column based on NaCl-induced size compaction and reduced electronegativities. Fig. 8 shows the effect of different NaCl (buffer B) gradient elutions on plasmid resolution. There is a general trend of increasing plasmid resolution with decreasing buffer B gradient across the buffer B gradient range tested. At 7 and 10%B/min, plasmid pcDNA3F and RNA appear as a single peak. This indicates that the increase in NaCl concentration is too abrupt and that the plasmid has too little time to separate from RNA. At 5%B/min, pcDNA3F and RNA are scarcely separated and pcDNA3F resolution is optimum at 3%B/min. It can also be seen that at <3%B/min, there is no significant improvement in resolution in addition to reduced plasmid yield. This is possibly due to a longer retention time which results in plasmid diffusion, band broadening thus lower plasmid yield.

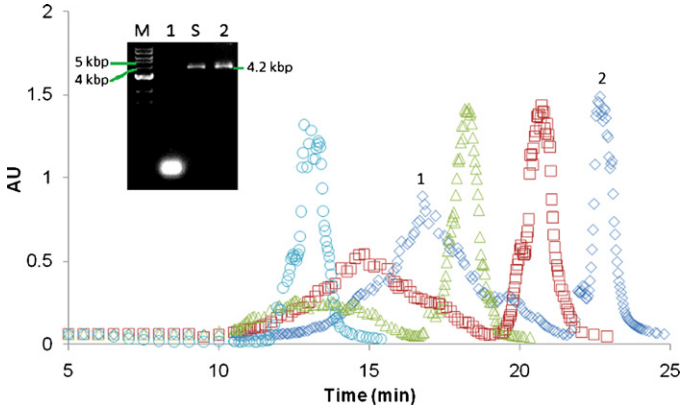

Fig. 7. Effect of ionic strength of binding buffer on plasmid retention. Buffer A (25 mM Tris–HCl, 2 mM EDTA, 0.3–0.7 M NaCl, pH 7). Buffer B (25 mM Tris–HCl, 2 mM EDTA, 1.0 M NaCl, pH 7). Flow rate: 1.0 mL/min; sample: 1.0 mL of clarified alkaline-lysed cell lysate; washing: 5 mL buffer A; gradient elution: 4% B/min. NaCl concentration in buffer A: 0.3 M (rhombus); 0.4 M (square); 0.5 M (triangle); 0.7 M (circle). Inset shows ethidium bromide gel electrophoresis of different samples taken at different peak elutions. Analysis was performed using 1% agarose in 100 mL TAE × 1 buffer, 0.5 μg/mL ethidium bromide at 65 V for 1.7 h. Lane M is 1 kbp DNA ladder; lanes 1 and 2 represent peaks 1 (RNA) and 2 (pcDNA3F) of the chromatogram; lane S is standard Maxiprep pcDNA3F.

Finding the right gradient of the eluting buffer proves to be essential in the chromatographic purification of plasmid DNA and the optimum buffer B gradient obtained in this study is plasmid-size specific. According to Smith et al. [4], when a specific gradient was used to elute a plasmid DNA of a different size, the resolution was considerably varied. They were unable to find a generic elution profile for plasmid DNA and discovered a size-dependent change in relative elution rates. They conducted plasmids (3.0, 5.5, 7.6 kbp) elution at different salt gradient slopes and measured the relative retention time (RRT) of supercoiled, linear and open circular plasmids.

3.6. Optimisation of pH conditions

Another important variable that plays an important role in ion exchange chromatography is pH condition of mobile phases. In this work, we investigated the effect of pH (2–12) on Zeta potential values of the monolith and plasmid DNA as well as on plasmid resolution. Generally, the plasmid remained negatively charged within the pH range tested (Fig. 9). Poly(GMA–EDMA)–DEA monolith displayed positive net charge at pH < 9, zero charge at pH 9, and negative charge at pH > 10. From these observations, it can be hypothesised that the plasmid will not bind to the lig-

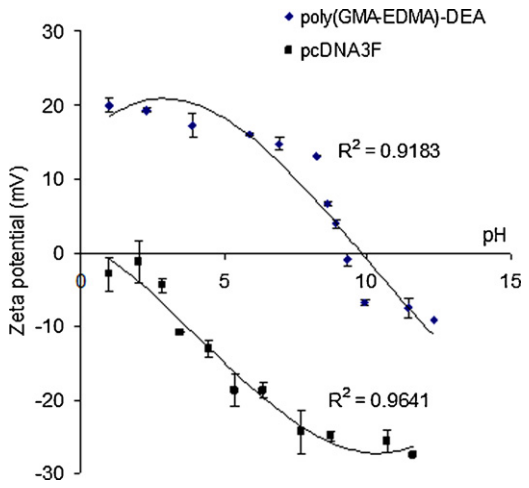

Fig. 9. Effect of buffer's pH on the Zeta potential of pcDNA3F and poly(GMA–EDMA)–DEA. Base buffer (25 mM Tris–HCl, 2 mM EDTA, 0 M NaCl, pH 7). Each data point represents the average of three replicates.

and at pH > 9 thus will move along with other impurities in the mobile phase uncaptured considering that the net charge does not take into account localized charged region. Optimum plasmid retention and resolution can be expected between pH 5 and 6 at which the difference in the magnitude of Zeta potential between the ligand and the plasmid is maximum. To verify these hypotheses, we conducted an anion exchange purification of plasmid-containing cell lysates at different pH values of the mobile phases.

It can be seen from Fig. 10 that at pH 9 and 10, there is no plasmid resolution since both plasmid and ligand are negatively charged. In this case, plasmid forms part of the flowthrough and co-elutes with the impurities namely RNA, nicked plasmids, proteins and lipopolysaccharides. Plasmids are best resolved from RNA at pH 6 as evident from Fig. 10 and Table 1. Under this pH value, plasmids are high negatively charged and have a strong attraction towards the positively charged anion exchange matrix thus higher retention time. In addition to that, it is speculated that under the same pH condition, other impurities mainly RNAs, proteins, gDNAs and nicked plasmids are also negatively charged but their magnitudes are substantially lower than that of supercoiled plasmids. As a consequence, plasmids and impurities can be separated during NaCl gradient elution in the order of increasing negative charge and retention time. These trends of plasmid retention as a result of pH

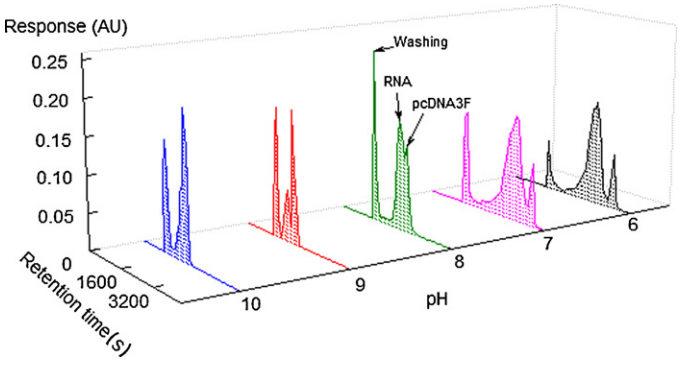

Fig. 10. Effect of pH on plasmid resolution. Flow rate 0.6 mL/min. Buffer A (25 mM Tris–HCl, 2 mM EDTA, 0.2 M NaCl). Buffer B (25 mM Tris–HCl, 2 mM EDTA, 1.0 M NaCl). Sample: 0.5 mL of clarified alkaline-lysed cell lysate. Washing, 30 CVs of buffer A; gradient elution, 4% B/min.

Table 1
Plasmid–RNA resolution (Rs) at different chromatographic conditions.

pH	6	7	8	9	10
Rs	*0.81*	*0.69*	*0.51*	*0*	*0*
% Buffer B/min	1	3	5	7	10
Rs	*0.73*	*0.85*	*0.43*	*0*	*0*
% Porogen	50	60	65	70	80
Rs	*0.52*	*0.75*	*0.89*	*0.65*	*0.6*
Buffer A ionic strength (M)	0.3	0.4	0.5	0.7	
Rs	*0.9*	*1.06*	*1.03*	*1.15*	

Rs = (T1 − T2)/0.5(W1 + W2), where T1: retention time of RNA (s), T2: retention time of pcDNA3F (s), W1: peak width of RNA (s), W2: peak width of pcDNA3F (s). All Rs values have p values <0.05.

conditions also agree with the studies done by Bencina et al. [22]. They studied the effect of pH of the mobile phase between 7 and 12. Retention of plasmids on a DEAHP (weak anion-exchanger) column significantly decreased at higher pH values. They concluded that the decrease in plasmid retention was attributed to DEAHP groups since the pH was not expected to significantly influence the charge on the plasmids. In this study however, we found out that the surface charge of both plasmid and anion exchange groups were significantly affected by pH as evident from Fig. 9 and were responsible for the plasmid retention.

4. Conclusions

This work describes the optimisation of process variables for the purification of plasmid DNA (pcDNA3F) using anion exchange monolithic chromatography techniques. This work concludes that plasmid separation can successfully be achieved simply by optimising ligand functionalisation temperature, mobile phase flow rate, monolith pore size, buffer pH, ionic strength of binding buffer and buffer gradient elution slope. Temperature greatly affects the amount of ligands attached to the base monolith matrix and optimum functionalisation can be carried out at 60 °C for 24 h. Sharp, symmetrical and minimised band broadening can be achieved at a mobile phase flow rate of 0.6 m/min. Preferential plasmid adsorption and optimum resolution can be achieved by loading the clarified alkaline-lysed plasmid-containing cell lysate into 400 nm pore size of monolith in 0.7 M NaCl (pH 7) of binding buffer followed by increasing the NaCl concentration to 1.0 M at 3%B/min.

Acknowledgements

The authors would like to thank Monash University, Australia and Universiti Malaysia Sabah, Malaysia for the financial support to carry out this project.

References

[1] A. Eon-Duval, G. Burke, J. Chromatogr. B 804 (2004) 327.
[2] D.M.F. Prazeres, T. Schluep, C. Cooney, J. Chromatogr. A 806 (1998) 31.
[3] F. Sousa, M.F. Duarte, Prazeres, J.A. Queiroz, Trends Biotechnol 26 (2008) 518.
[4] C.R. Smith, R.B. DePrince, J. Dackor, D. Weigl, J. Griffith, M. Persmark, J. Chromatogr. B 854 (2007) 121.
[5] M.M. Diogo, J.A. Queiroz, D.M.F. Prazeres, J. Chromatogr. A 1069 (2005) 3.
[6] M.W. Roberts, C.M. Ongkudon, G.M. Forde, M.K. Danquah, J. Sep. Sci. 32 (2009) 2485.
[7] J. Urthaler, R. Schlegl, A. Podgornik, A. Strancar, A. Jungbauer, R. Necina, J. Chromatogr. A 1065 (2005) 93.
[8] C.P. Bisjak, R. Bakry, C.W. Huck, G.K. Bonn, Chromatographia 62 (2005) S31.
[9] H.Y. Aboul-Enein, I. Ali, H. Hoenen, Biomed. Chromatogr. 20 (2006) 760.
[10] I. Ali, V.D. Gaitonde, H.Y. Aboul-Enein, J. Chromatogr. Sci. 47 (2009) 432.
[11] H.Y. Aboul-Enein, I. Ali, Talanta 65 (2004) 276.
[12] I. Ali, H.Y. Aboul-Enein, Anal. Lett. 37 (2004) 2351.
[13] I. Ali, F.E.O. Suliman, H.Y. Aboul-Enein, LC–GC 27 (2009) 22.
[14] http://www.biaseparations.com/products.asp?FolderId=251&TabId=322 (accessed 15.05.10).
[15] S.H. Ngiam, Y.H. Zhou, N.J. Turner, N.J. Titchener-Hooker, J. Chromatogr. A 937 (2001) 1.

[16] A. Zochling, R. Hahn, K. Ahrer, J. Urthaler, A. Jungbauer, J. Sep. Sci. 27 (2004) 819.
[17] C.S. Lengsfeld, T.J. Anchordoquy, J. Pharm. Sci. 91 (2002) 1581.
[18] S. Kong, N. Titchener-Hooker, M.S. Levy, J. Membr. Sci. 280 (2006) 824.
[19] M.K. Danquah, G.M. Forde, Chem. Eng. J. 140 (2008) 593.
[20] A.V. Delgado, F. Gonzalez-Caballero, R.J. Hunter, L.K. Koopal, J. Lyklema, Pure Appl. Chem. 77 (2005) 1753.
[21] G.S. Manning, Biopolymers 19 (1980) 37.
[22] M. Bencina, A. Podgornik, A. Strancar, J. Sep. Sci. 27 (2004) 801.